

ION TRAJECTORY SIMULATIONS IN A MALDI ION SOURCE FOR PARTICLE ACCELERATORS

J.A.M. Pereira^{1*}; W.S. Santos²; A.M. Luiz²; N.V. de Castro Faria²

¹ Laboratório de Instrumentação e Partículas, IF – USP, CP 66318, 05315-970, São Paulo, Brasil

² Laboratório de Colisões Atômicas e Moleculares, IF – UFRJ, CP 68528, 21941-972, Rio de Janeiro, Brasil

Received: August 3, 2004; Revised: April 28, 2005

Keywords: MALDI, delayed extraction, electrostatic lenses.

ABSTRACT

This work is part of a project for the construction of a MALDI ion source. This source is to be attached to a TANDEM particle accelerator. Since the ions produced in the source must travel considerable distances ~ 2 m before entering the injection system of the accelerator, a set of electrostatic lenses is needed in order to gain high transmission. An investigation based on ion trajectory simulations carried out with the SIMION computer code was made. Calculations of the transmission and angular dispersion as function of the lens parameters are presented.

1. INTRODUCTION

In recent years, the desorption technique so called Matrix Assisted Laser Desorption Ionization (MALDI) have achieved great popularity receiving the Chemistry Nobel prize in 2002 [1]. Its ability to produce the desorption of very large intact molecules with high emission yields, combined with time-of-flight analysis, provides a powerful analytical tool that has been widely used as a proteomic technique [2].

In MALDI, a pulsed laser is used to bombard a composite solid. The energy deposition process induced by the laser light leads to ion ejection (or desorption) from the surface. The composite solid contains analyte molecules (proteins, for instance) embedded in a light absorbing substance (matrix). In general, a UV-laser is used and the UV absorbing substance is an aromatic compound. The desorbing ions have an initial kinetic energy distribution whose the mean value is in the order of 10 eV [3]. Therefore, they have to be accelerated in order to be detected. Commercial time of flight spectrometers use high voltage power supplies to generate accelerating electric fields leaving the ions with energies ~ 20 keV, appropriated for their detection. It happens that the detection efficiency diminishes for high masses since the high mass ion velocities, at 20 keV, are not sufficient to trigger the detector, usually a micro channel plate in a chevron arrangement.

As an illustration, figure 1 presents a MALDI spectrum of Insulin using 2,5 dihydroxybenzoic acid (DHB) as matrix obtained using a commercial spectrometer (Applied Biosystems - Voyager DE). One can see the presence of high mass

clusters of insulin and that the ion signal decline for the heavier clusters as consequence of their lower detection efficiency.

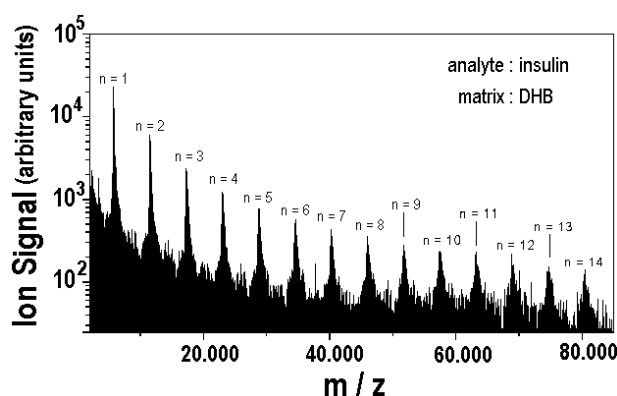


Figure 1 - MALDI spectrum of insulin. The variable n represents the number of insulin molecules in a given cluster.

In principle, a MALDI ion source attached to a particle accelerator can work as a high sensitivity time of flight spectrometer. After being accelerated to MeV energies, the high mass ($m > 100.000$ u) ions impact the detector with sufficient speed for detection. This MALDI-AMS system can potentially enlarge the mass range of MALDI analysis to a limit yet unknown. The acceleration to MeV energies also acts to improve the detection limit in the low mass range ($m < 100.000$ u) increasing the signal to noise ratio.

An ion source for such application needs a set of electrostatic lenses in order to guide the desorbed ions into the accelerator injection system with appropriate trajectories. The trajectory calculations were performed using the SIMION computer code [4].

2. PROCEDURES AND DISCUSSION

The simulated electrode geometry can be seen in figure 2 (out of scale). The system consists of a metal plate at potential V_1 , where the MALDI samples should be placed, a grid at potential V_2 for ion extraction, and the focusing elements: a metal ring at potential V_{ring} , a second grid to define the ground and two cylinders used as an Einzel lens at potential V_L (the second cylinder is grounded).

* jamp@fge.if.usp.br

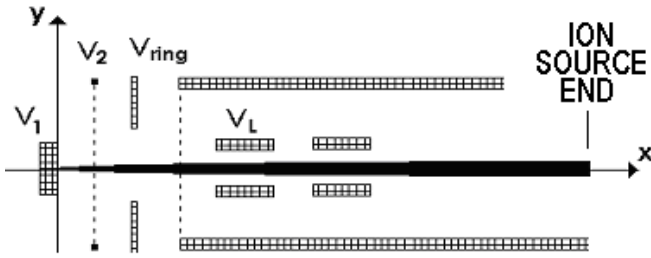


Figure 2 - Set of electrodes used in the simulations.

For the simulations, the extraction electrodes potentials were chosen as $V_1 = 10$ kV, $V_2 = 8$ kV and the focusing system, composed by the ring and the Einzel lens, were used independently. The dimensions the focusing system are: ring diameter = 1 cm, lens diameter = 1.8 cm, lens width = 1 cm with a gap of 1 cm between the two cylinders. Figure 3 shows an example of the simulation procedure for the determination of the trajectories. The simulations were carried out for mass 100.000 u with trajectories starting at $y = x = 0$, with initial angles from -90 to 90 degrees, with respect to the x - axis, and for initial energies, E_0 , of 5eV, 10eV and 20eV.

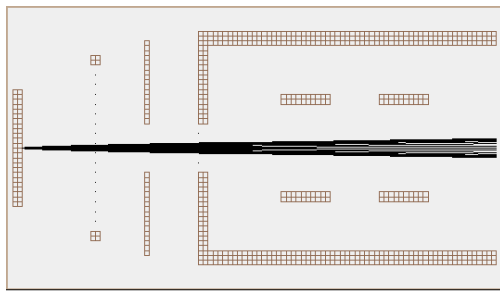


Figure 3 – Example of the simulation output with values: $E_0 = 5$ eV, $V_{ring} = 5.0$ kV and $V_{lens} = -3.0$ kV.

The SIMION code computes the electric potential over all space for a given geometry and applied voltages on the electrodes. It also permits the calculation of ion trajectories as function of a given set of initial conditions. The program outputs the coordinates, angles, time of flights and energies corresponding to each trajectory at the ion source end. In order to determine the transmission into the accelerator injection system, composed by a pair of deflection plates and an Einzel lens with an aperture of ~ 5 cm (radius $R \sim 2.5$ cm) located ~ 2 m away from the ion source end, an additional calculation needs to be done. The remaining path, between the ion source end and the injection system entry, is a straight line defined by $y = y_0$ and the final angle θ_0 given by the simulation. If $Y = y_0 + L \cdot tg\theta_0 < R$, with $L \sim 2$ m being the distance between the ion source end and the injection system entry, a successful transmission occur (fig. 4).

The values of Y are shown as a function of the initial angles in figure 5 for $E_0 = 20$ eV and for different values of V_{ring} by setting $V_L = 0$. According to the above procedure the transmission coefficient, T , was computed by counting the number of data points in the interval from $Y = -2.5$ cm and $Y = +2.5$ cm for all initial angles.

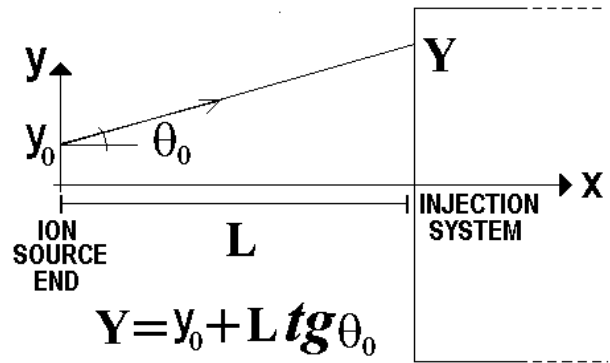


Figure 4 - Trajectory between the ion source end and the injection system entry. Successful transmission occur if $Y < R$ with R being the radius of the accelerator Einzel lens aperture.

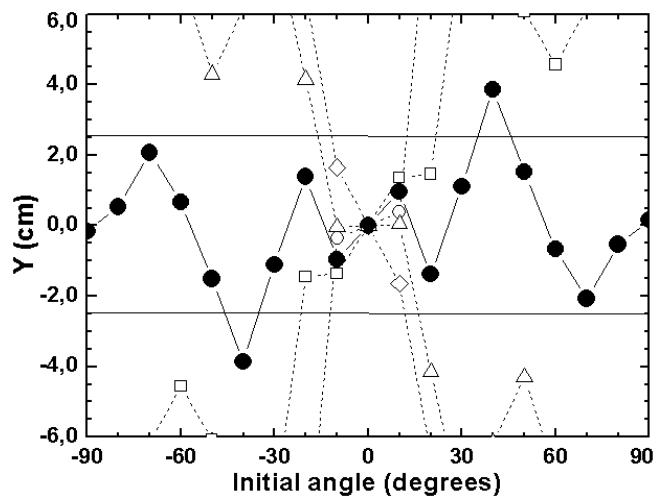


Figure 5 - Values of Y for different values of the potential V_{ring} : $\square = 4.5$ kV, $\bullet = 6.0$ kV and $\Delta = 7.5$ kV

One can observe a 90% transmission coefficient for $E_0 = 20$ eV if $V_{ring} = 6.0$ kV is chosen. Similar results are obtained for $E_0 = 5$ eV and 10 eV and the computed transmission coefficients are show in figure 6 as function of V_{ring} . At this point, it should be stressed that one trajectory does not correspond necessarily to one ion. The ion emission processes do not produce all the ejection initial angles presented in figure 5. Another criterion, considering the ejection angular distribution, may be used in the calculations. Usually, the angular distribution of the ions at emission is assumed to be proportional to $\cos^n \theta_i$ [5].

However, if the trajectory transmission is 100% the ion transmission will certainly be 100% too irrespective to the shape of the angular distribution of emission. So the option to work with the transmission of trajectories was adopted. An optimal transmission coefficient is achieved by setting $V_{ring} = 6.0$ kV. The broadening of the transmission peak for lower E_0 values indicates that a higher accuracy is needed in setting the potential on the metal ring for focusing the trajectories corresponding to higher initial kinetic energies. It is also worth to calculate the angular dispersion of the trajectories for different values of V_{ring} . This is shown in figure

7 where, as expected, one sees that a minimum dispersion is achieved when a maximum transmission is observed.

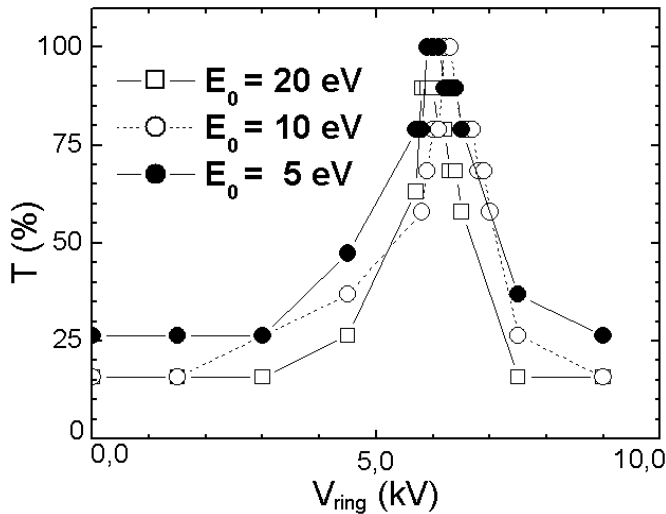


Figure 6 - Transmission coefficients computed for the three considered initial kinetic energies.

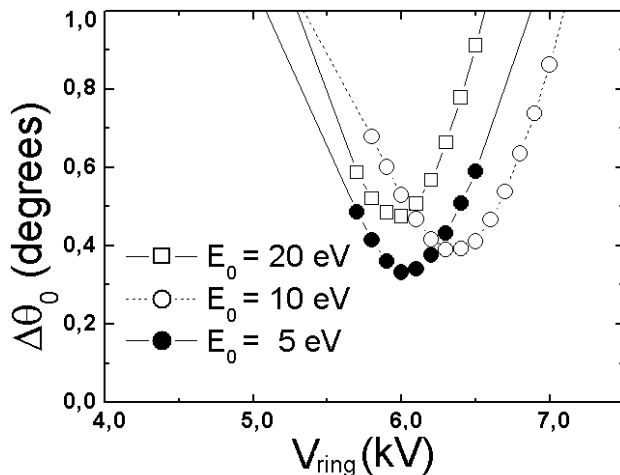


Figure 7 - Angular dispersion as a function of V_{ring} .

Letting $V_{ring}=6.0$ kV, the variation of V_L was analyzed within the same procedure. The transmission coefficients are presented in figure 8 and the angular dispersions in figure 9.

The local minimum for $E_0=10$ eV is a consequence of the higher angular dispersion of the trajectories with initial kinetic energy of 10 eV and $V_{ring} = 6.0$ kV (see figure 7). This should disappear if the value of V_{ring} is shifted to 6.1 kV or 6.2 kV. This is also appearing in the angular dispersions presented in figure 9 where, for $E_0=10$ eV, the local maximum of the angular dispersion corresponds to the local minimum of the transmission coefficient. The optimal V_L value corresponds to the minimum angular dispersion. In the present case, this is accomplished for $V_L=-5.0$ kV, for $E_0=20$ eV and $V_L = -9.0$ kV for the other two cases. A convenient choice would be $V_L = -7.5$ kV since for this

value the transmission coefficient is maximum for all cases (see figure 8). Letting $V_{ring} = 6.0$ kV and $V_L = -7.5$ kV, the trajectories are almost parallel to the axis of the injection system Einzel lens which is an optimal situation for the ions to enter the accelerator.

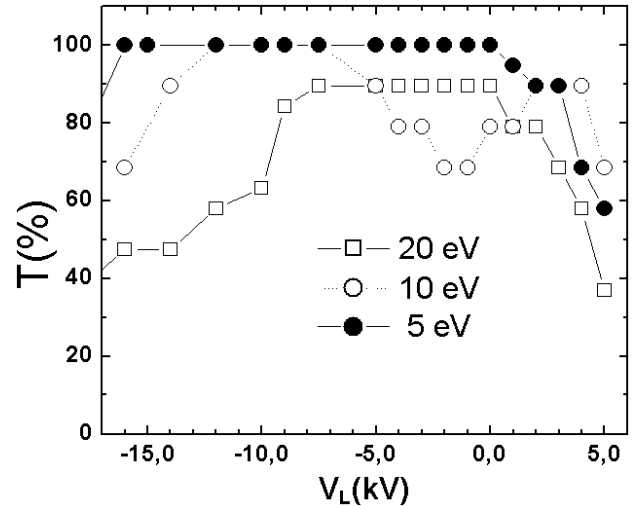


Figure 8 - Transmission coefficients as a function of V_L .

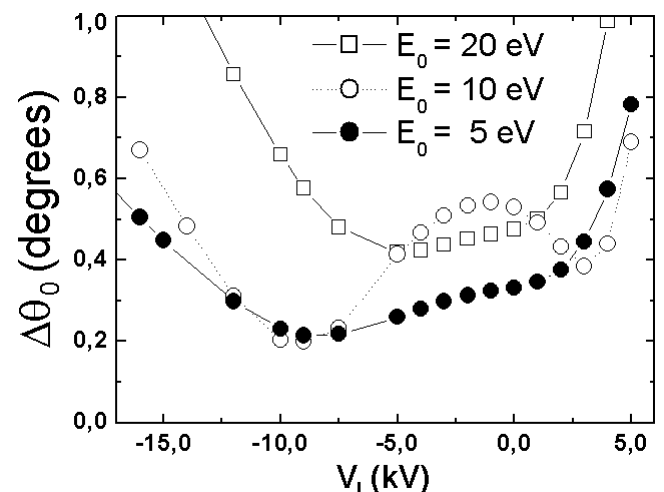


Figure 9 - Angular dispersion as a function of V_L .

3. SIMULATIONS FOR DELAYED EXTRACTION

Further investigations were carried out considering the delayed extraction technique. The delayed extraction was introduced in MALDI in order to increase the mass resolution of time of flight instruments and is available in commercial spectrometers [6]. The operational principle of delayed extraction is the free expansion of the ion cloud generated by the laser pulse impact. This is done setting the potential difference between the sample (V_1) and the first grid (V_2) equals to zero ($V_1 = V_2$ in figure 2) and certainly has an effect on the transmission and angular dispersion. After a given time interval, τ , the sample potential, V_1 , is suddenly increased by ΔV (8 kV to 10 kV in our case) and the extraction electric field is established. As a result, the ions emitted

with low kinetic energies receive larger impulses thus compensating the initial kinetic energy difference at emission. The time delay τ can be chosen to minimize the time of flight dispersion due to the initial kinetic energy distribution of a given ion.

The simulation of this extraction mode with SIMION is not straightforward since the program does not allow time dependent voltages. This was performed letting the ions initial positions vary according to their initial velocities, v_0 , angles, θ_i , and the time delay, τ . Accordingly, the starting points of the trajectory simulations are given by $x = v_0 \cos \theta_i \tau$ and $y = v_0 \sin \theta_i \tau$. This was done for $E_0 = 10$ eV, $V_{\text{ring}} = 6.0$ kV, for V_L varying from -9.0 kV to 6.0 kV and letting τ assuming values from zero to $5.0 \mu\text{s}$. The results are shown in figure 10, for the transmission coefficient, and figure 11, for the angular dispersion.

In spite of the spatial dispersion inherent to the delayed extraction method, it is still possible to work with a 100% transmission. As in the previous cases, a high transmission coefficient correlates with low angular dispersions as can be seen comparing figures 10 and 11. The best value for V_L in this case would be $V_L = -5.0$ kV which optimize the values of the transmission coefficient and angular dispersion for a range of $4 \mu\text{s}$ in delay time.

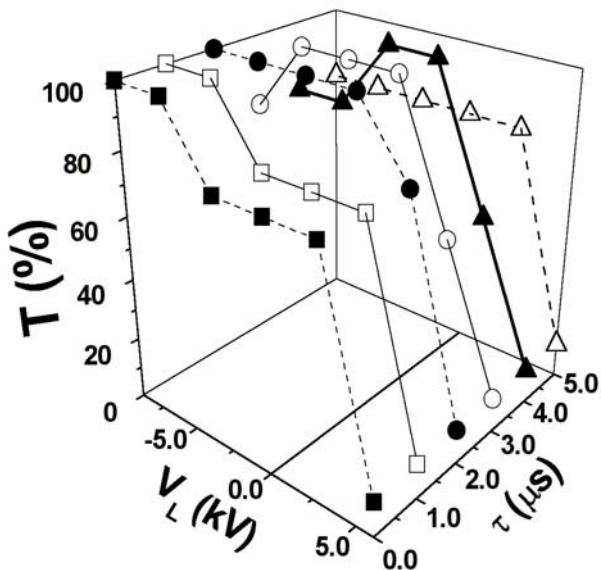


Figure 10 - Transmission coefficients computed for the delayed extraction mode.

4. CONCLUSION

Numerical calculations were performed to find an optimal trajectory configuration in the ion source. The criteria used to adjust the operational conditions of the electrodes were the transmission coefficient and the angular dispersion. The maximization of the transmission coefficient was achieved by varying the values of V_{ring} while the minimization of the

angular dispersion was accomplished by varying the potential V_L . The optimal values were found to be $V_{\text{ring}} = 6.0$ kV and $V_L = -7.5$ kV. The introduction of the delayed extraction changes the optimal values of the electrode voltages. Although, it is still possible to work with high transmission if $V_L = -5.0$ kV is chosen. The inclusion of a cos-like angular distribution for the ion emission will change the transmission coefficient and angular dispersion values. However, it is not expected that the electrode voltage values presented here will change drastically since they were obtained by optimizing the number of transmitted trajectories by making the transmission coefficient to be close as possible to 100%.

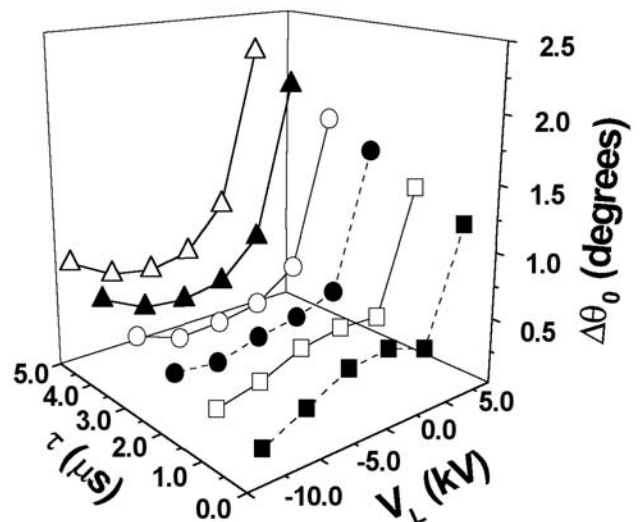


Figure 11 - Angular dispersion computed for the delayed extraction mode

5. ACKNOWLEDGEMENTS

This work have been financially supported by FAPERJ with the program *Cientista Jovem do Nosso Estado*

6. REFERENCES

1. <http://www.biomedcentral.com/news/20021211/03/>.
2. RAPPSILBER, J.; MONIATTE, M.; NIELSEN, M.L.; PODTELEJNIKOV, A.V.; MANN, M., *Int. J. of Mass Spectr. and Ion Proc.* 226 (2003) 223.
3. GLUCKMANN, M.; KARAS, M., *J. Mass Spectrom.* 34 (1999) 467.
4. <http://www.simion.com>.
5. JOHNSON, R.E.; LEBEYEC, Y., *Int. J. of Mass Spectr. and Ion Proc.* 177 (1998) 111.
6. FOURNIER, I.; BRUNOT, A.; TABEL, J.C.; BOLBACH, G., *Int. J. Mass Spectr.* 213 (2002) 203.